Electrochimica Acta xxx (2015) xxx–xxx

Contents lists available at ScienceDirect

Electrochimica Acta

journal homepage: www.elsevier.com/locate/electacta

Protection and functionalization of AISI 316 L stainless steel for orthopedic implants: hybrid coating and sol gel glasses by spray to promote bioactivity

S.A. Omar, J. Ballarre, S.M. Ceré[1,*]

División Electroquímica y Corrosión, Facultad de Ingeniería, Universidad Nacional de Mar del Plata—INTEMA, CONICET, J. B. Justo 4302, B7608FDQ Mar del Plata, Argentina

ARTICLE INFO

Article history:
Received 13 August 2015
Received in revised form 4 January 2016
Accepted 7 January 2016
Available online xxx

Keywords:
stainless steel
coatings
bioactive glass

ABSTRACT

This work presents the synthesis and deposition of hybrid sol-gel coating applied on AISI 316Lstainless steel by dipping with the aim of providing corrosion protection to the substrate. On the top of this coating a potentially bioactive glass (58S) made also by sol gel method with tetraethoxysilane (TEOS), triethyl phosphate (TEP) and calcium nitrate as precursors, was applied by spray technique. This method allows the creation of a wide distribution of particles sizes on the target. Coatings were characterized by profilometry and optical and electronic microscopy. The surface integrity and corrosion resistance of the coatings in time is analyzed by electrochemical tests in simulated body fluid (SBF).It is observed some kind of detrimental effect regarding the corrosion behavior between the bioactive dots and the underneath coating. Nevertheless the entire system results promising for further investigation since the addition of 58S bioactive particles by spray method results appealing as it is a simple way to generate bioactive points on the implant surface.

1. Introduction

Biological environment is known for being aggressive for the materials which are in contact with it. This makes corrosion protection an essential matter to analyze when selecting an intracorporeal permanent implant. A widely spread used material in Latin America for surgical purposes is the AISI 316L stainless steel even it has the limitation of being sensitive for localized corrosion and present poor osseointegration. Here is where surface modification becomes an appealing strategy to apply. Even though there are many techniques to improve material's surface, coatings highlights in this field as they generate a new surface which will interact with the surrounding media acting as a barrier for ions migration.

In matter of coatings, the organic-inorganic hybrid materials have taken the attention from academic and technological institutes due to the unusual combination of physical and chemical properties which are capable to exhibit [1,2]. Pure inorganic films have limitation such as micro cracks, residual porosity and the formation of very thin films, the incorporation of non-hydrolysable groups has reduced some of these limitations [3–5]. The final hybrid material consists in a Si-O-Si network modified with some organic groups. The traditional way to apply this kind of hybrid coating is by dipping, as this technique can arise to homogeneous and crack free coatings with excellent corrosive properties.

However, the application of a protective coating improves only one aspect to fulfill in the use of AISI 316L implants. Osseointegration cannot take place between materials which show no sign of bioactivity and here another strategy requires to be chosen. An alternative to promote bioactivity are the bioactive glasses, since they have the ability to bond with living tissues forming an apatite layer. If they are made by sol-gel, they have also the advantage of high degree of purity and good homogeneity [6]. The sol gel route starts with the preparation of a sol, obtained by mixing in aqueous medium different precursors (in acid or basic catalyst), like tretraethyl orthosilicate (TEOS), triethyl phosphate (TEP), and calcium nitrate tetrahydrate as sources of SiO_2, P_2O_5 and CaO, respectively. After hydrolysis and polycondensation that take place at room temperature, a gel is obtained which can be aged, dried and stabilized at different conditions [7].

In this work we propose to generate a protective sol gel layer on stainless steel by dipping and then to functionalize it with a sol gel glass from the $CaO\text{-}SiO_2\text{-}P_2O_5$ system, applying it by a versatile and simple method as it is spray deposition. The aim of this surface

* Corresponding author. Fax: +54 223 481 0046.
E-mail address: smcere@fi.mdp.edu.ar (S.M. Ceré).
[1] ISE active member.

http://dx.doi.org/10.1016/j.electacta.2016.01.051
0013-4686/

treatment is to generate bioactive points spread on the surface together with the corrosion protection produced for the underneath coating.

2. Experimental

The procedure followed to obtain the samples for further evaluation in sketched in Fig. 1.

2.1. Sol gel protective layer

Stainless steel AISI 316L (SS, Roberto Cordes, Argentina) was used as substrate. SS was polished with cloth to get a bright finished, then cleaned and degreased with isopropyl alcohol in ultrasound and finally coated with a hybrid organic-inorganic coating. This hybrid organic-inorganic sol (TMS) was prepared with tetraethoxysilane (TEOS, 99% Sigma Aldrich), methyltriethoxysilane (MTES, 98% Sigma Aldrich) and colloidal silica suspended in water (SiO_2, LUDOX 40 wt%, Dow). The molar ratio of the alkoxides was kept constant (TEOS/MTES = 40/60) and the addition of colloidal silica was 10 per cent in moles respect with the total amount of SiO_2. The final silica concentration was 200 g/L and the water amount was kept stoichiometric. This synthesis was performed in acidic catalysis. Coating was performed by dip coating with a withdrawal speed of 20 cm/min. A thermal treatment at 450 °C for 30 minutes in air atmosphere was carried out to consolidate the coated system (referred as SS + TMS).

2.2. Sol gel bioactive layer

58S glass (60 mol% SiO_2, 36 mol% CaO, 4 mol% P_2O_5) was obtained using tetraethoxysilane (TEOS, 99% Sigma Aldrich), triethyl phosphate (TEP, 99% Sigma Aldrich) and calcium nitrate tetrahydrate ($Ca(NO_3)_2.4H_2O$, Biopack) as precursors, with a volume ratio of $H_2O/HNO_{3(V)} = 6$. Bioactive spots on the new substrate (SS_TMS) were applied by spray, using 400 mm/s of speed rate, 23 cm distance between the spray gun and the target and a variable pressure (0.8 or 1 Bar) for the fresh and aged sol respectively.

Half of the prepared sol was immediately applied by spray method (fresh sol, pressure: 0.8 Bar) on the coated substrates and transferred to an oven at 70 °C for drying. Gelation was observed to occur within a few hours at that temperature. The other half sol was left for a 24 hours aging process at room temperature (aged sol, called "RT, 24h" throughout the manuscript) in a tight container, before being applied by spray technique (pressure: 1 bar) on coated substrates and then submitted to a drying process at 70 °C in the oven.

After having two types of samples (SS_TMS with 58S either fresh or aged), samples were thermally treated in an oven at 450 °C during 3 hours in air atmosphere in order to eliminate nitrates and to allow calcium to diffuse into the silica network [8].

As a summary, two kinds of samples were obtained which notation is shown below:

- SS_TMS_58S: coated samples with TMS on SS (thermal treated at 450 °C for 30 minutes) + spots of 58 S glass made using fresh sol (72 h drying at 70 °C + 3 h thermal treated at 450 °C in air).
- SS_TMS_58S-a: coated samples with TMS on SS (thermal treated at 450 °C for 30 minutes) + spots of 58 S glass made using aged sol gel (RT, 24 h) (72 h drying at 70 °C + 3 h thermal treated at 450 °C in air).

2.3. Sample superficial characterization

The thickness and homogeneity of the protective layer was evaluated with a profilometer KLA Tencor (Alpha-Step D-100, US).

Both conditions (SS_TMS_58S and SS_TMS_58S-a) were analyzed *in vitro* by immersion in simulated body fluid (SBF) which contains similar inorganic concentration of ions than the human plasma (Table 1). The samples were immersed in SBF for 17 days,

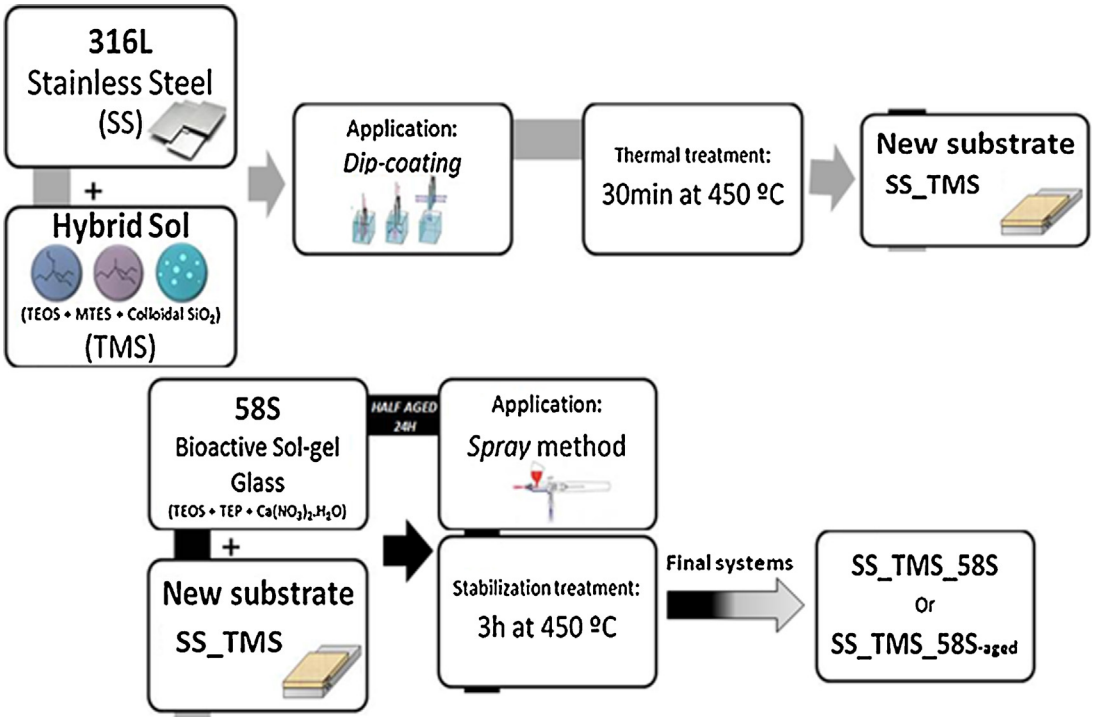

Fig. 1. Flowchart summary of the steps followed to prepare samples. Grey path leads to the protective layer and black path gets the bioactive layer.

Please cite this article in press as: S.A. Omar, et al., Protection and functionalization of AISI 316L stainless steel for orthopedic implants: hybrid coating and sol gel glasses by spray to promote bioactivity, Electrochim. Acta (2016), http://dx.doi.org/10.1016/j.electacta.2016.01.051

Table 1
Simulated body fluid chemical composition in g.L^{-1} [9].

NaCl	KCl	$CaCl_2$	$MgCl_2.6H_2O$	K_2HPO_4	$NaHCO_3$	$(CH_2OH)_3CNH_2$
8.053	0.224	0.278	0.305	0.174	0.353	6.057

*pHadjustedto7.25±0.05withHCl.

and kept at 37 °C in a furnace. In all cases, samples without immersion procedure were used as control.

Particle size, distribution and coatings visual integrity were examined by scanning electronic microscopy (SEM) with JEOL JSM-6460LV (Japan) equipment, prior to immersion and after 17 days in SBF.

In order to analyze *in vitro* bioactivity and 58S glass dissolution, micro-Raman assays were conducted on immersed samples in SBF for 17 days at 37 °C using an Invia Reflex Confocal (Renishaw RM 2000, UK) with a 785 nm wavelength laser, at 50% intensity in a window from 400 to 1400 cm^{-1}, with 15 accumulations and 1 second of exposition per spectrum.

2.4. Electrochemical techniques

Electrochemical assays were carried out in a GAMRY Ref 600 electrochemical unit (Gamry, USA) with a conventional three electrode cell. The reference electrode was a saturated calomel electrode (SCE, Radiometer Copenhagen 0.241 vs Standard hydrogen electrode, SHE), a platinum wire as a counter electrode and the stainless steel, either bare or coated as working electrode. SBF was used throughout the experiments.

Potentiodynamic polarization curves were scanned from open circuit potential after stabilization to 1.2 V or a current density of 4 10^{-3} A cm^{-2} at a rate of 2 mV/s. Electrochemical impedance spectroscopy (EIS) tests were registered at the corrosion potential (Ecorr) with amplitude of 0.005 V rms sweeping frequencies from 20000 to 0.02 Hz. Impedance data fitting was performed using Zplot software [9].

3. Results and discussion

Fig. 2 shows the results obtained from the profilometry assays. It can be seen that the SS_TMS coating applied by dip-coating presented a thickness of 1.2 ± 0.1 μm. The rise in the profilometry curve is usually associated to materials' accumulation in the transition zone.

Scanning electron microscopy photos at the initial condition and after an immersion process are shown in Fig. 3. Samples SS_TMS_58S-a showed most of the particles cracked, before immersion meanwhile SS_TMS_58s showed round, agglomerated

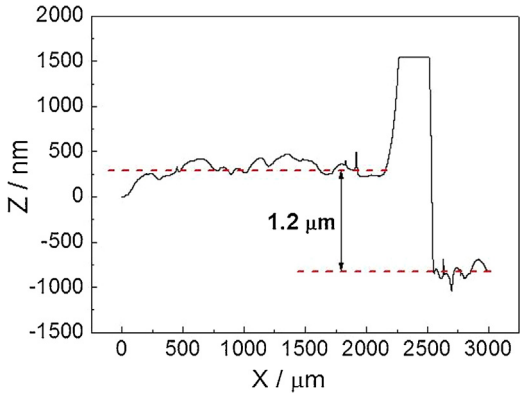

Fig. 2. Profilometry curve obtained for the TMS coating.

but well distributed particles on the substrate before immersion. When considering samples after immersion, both showed substantial dissolution of the particles and some precipitates on the surface. EDS results showed that elements such as Ca, Na, P, Cl and Si were present. However, it is not correct to assume either presence or absence of hydroxycarbonated apatite (HCA) as that only implies an elemental analysis. No presence of Ca and P related compounds was found in the bare stainless steel substrate after immersion in SBF.

The presence of the different compounds in the layers and their evolution with immersion time were analyzed by micro Raman spectroscopy. The technique is a powerfull one to analyze remain particles in the coatings and new deposits pre and post immersion in simulated body fluid. Fig. 4 shows Raman spectra of SS_TMS_58S and SS_TMS_58S-a before immersion and after 17 days of immersion in SBF. The typical spectrum of the hybrid silica based TEOS-MTES coating was added as comparison. As the bare substrate (stainless steel 316L) do not present any deposits at all, the spectra is not shown [10]. Table 2 shows the individual bands and the corresponding vibrational position in the Raman spectra of the different types of sol gel glass studied.

The bands related with Si-O ring bonds of the tetrasilanes are present at 485, 606, and 794 cm^{-1} [11,12]. The 606 cm^{-1} band is associated with the Si-O ring defects [13]. The effect of MTES presence in the TMS layer can be denoted by the —CH_3 rocking at 1169 cm^{-1} [14] and the Si-CH_3 stretch at 1242 cm^{-1} [15].

The SS_TMS_58S coated systems (without and with aging treatment of the 58S glass) without immersion in SBF, also present some of the typical Si-O and Si-CH_3 bands denoting the coating presence. The glass particles show characteristic bands related with a silica gel doped with phosphorus made by TEOS and TEP [11]. were some silanol double bonds are already present, showing that the gel is still hydrolyzing and policondensating. The effect of calcium nitrate addition can be analyzed by the 1053 cm^{-1} band, where this position denotes that the nitrate ions are surrounded by water molecules, and that they are also coordinated by Ca cations [16]. The presence of a band around 1060 cm^{-1} can be associated with the presence of NO_3^- coordinated with calcium cations [17] and with the presence of asymmetric stretching P-O in PO_4^{3-} [18]. It can be seen that when the aging treatment was done, the nitrates are not bonded to the structure (free ions in the solution), and there are also phosphates as a part of the gel structure. Ca ions enter in the silica network by thermal migration for treatment temperatures higher than 350 °C, and the remaining nitrates are expected to be driven off with temperatures above 550 °C [19,20]. As the thermal treatment temperature chosen was 450 °C it was not enough to eliminate all the nitrates in the glass structure, and so they remain in the glass. After 17 days of immersion in SBF no significant changes were found comparing both systems (SS_TMS_58S and SS_TMS_58S-a). After the immersion time, the nitrate bands decrease in intensity in both cases. Also the band related with defects in the Si-O rings is stronger (606 cm^{-1}) since it is overlapped with O-P-O second vibration mode in phosphate glasses [21]. The higher intensity of the peaks could be related with the presence of a phosphate-rich deposit on the coatings surface, after 17 days of immersion. The 761 and 1184 cm^{-1} are bands related with Si-O-Si asymmetric bond vibrations in silica gels treated below 500 °C [22], and the 1297 cm^{-1} band is are related with phosphate vibrations [11,23] in the existing structure or in the new surface deposits. There is also a strong signal related with Si-OH (912 cm^{-1}) [11], indicating the formation of a silanol layer on top of the glass. This fact can be considered as the beginning of a bioactivity signal and hydroxyapatite formation [24].

Fig. 5 shows the polarization curves obtained for the coated samples at the initial immersion time and after 17 days of immersion. It can be observed that TMS remains without

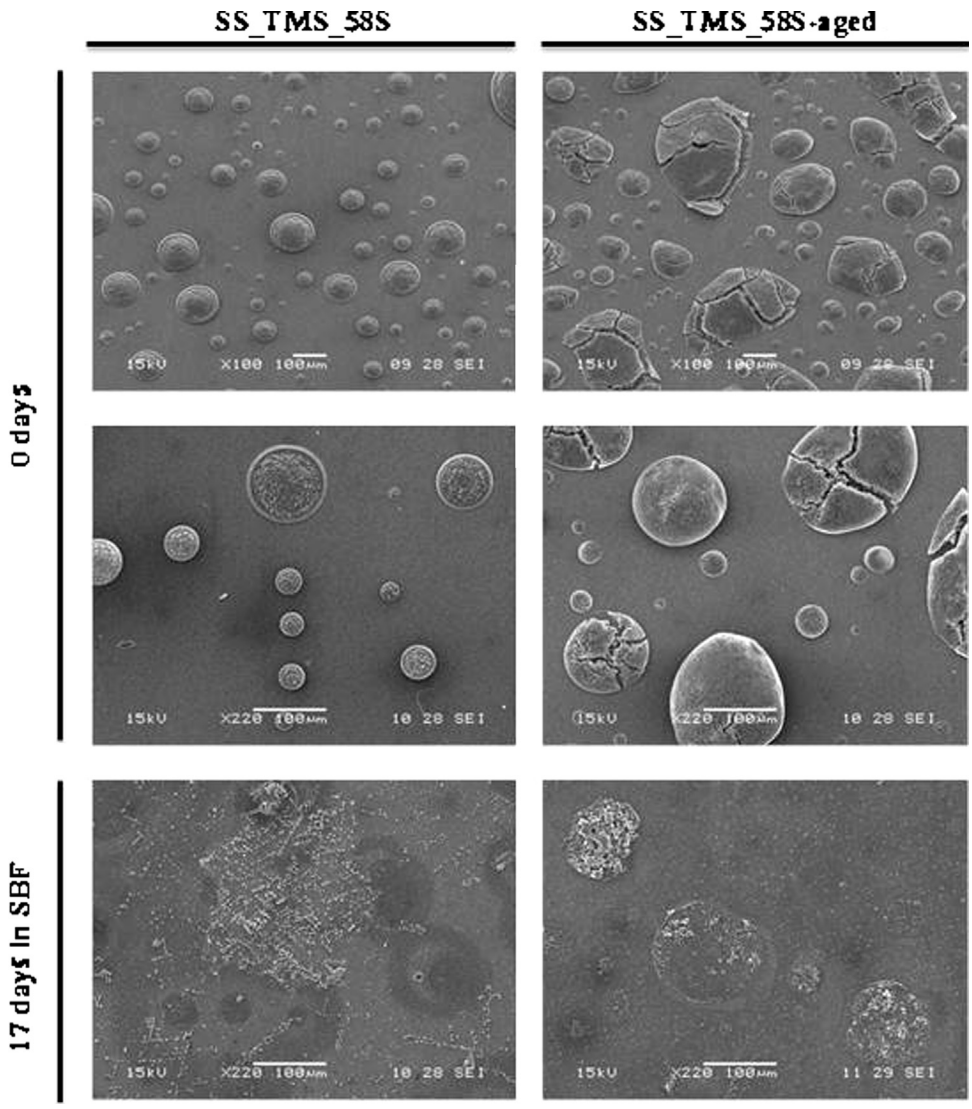

Fig. 3. SEM images of the coated samples before immersion at two magnifications and after 17 days immersion in SBF.

remarkable changes after immersion but the other coatings shows signs of degradation since higher current density is observed after immersion in SBF. This fact is related to a higher substrate exposed area and thus with a more deteriorated coating [25].

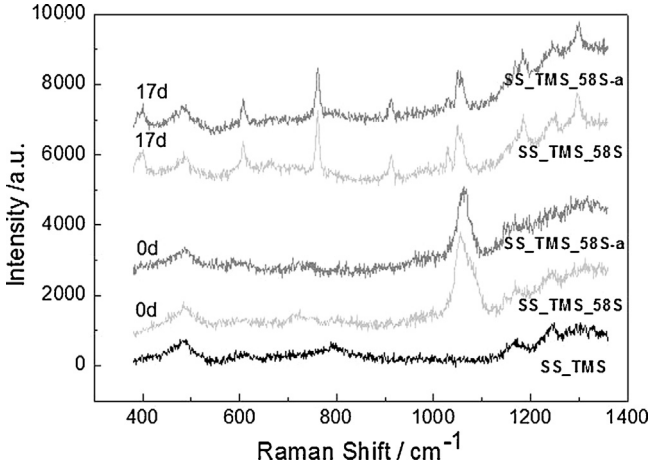

Fig. 4. Raman spectra of SS_TMS_58S and SS_TMS_58S-a before and after 17 days of immersion in SBF. The spectrum of the hybrid silica based TEOS-MTES coating was added as comparison.

The impedance spectra recorded for all samples at initial conditions (immediately after immersion) and after immersion times (17 days) in SBF at 37 °C are shown in Fig. 6. Bode representations of impedance assays shows that the TMS layer acts as a good barrier for the bare metal. However, the addition of bioactive particles results in a decrease of total impedance modulus, being more significance for the sample with 58S aged. Bode representation of the phase angle evidences that the SS_TMS samples have capacitive behavior with constant angles close to 90° and no deterioration after immersion. The incorporation of particles induces some degree of worsening on the lower layer. The effect is more pronounced for the SS_TMS_58S-a where the defects observed in the particles after thermal treatment (see Fig. 3) seems to affect the lower layer too as it is evidenced in the drop of the impedance modulus and the decrease in the phase angle in the high frequency region. This effect is much less pronounced for the SS_TMS_58S condition. After 17 days of immersion in SBF, both coating containing particles show significant deterioration meanwhile the coatings without particles (SS_TMS) remains almost constant. SS_TMS_58S and SS_TMS_58S-a coatings show impedance modulus similar to the bare material

Please cite this article in press as: S.A. Omar, et al., Protection and functionalization of AISI 316L stainless steel for orthopedic implants: hybrid coating and sol gel glasses by spray to promote bioactivity, Electrochim. Acta (2016), http://dx.doi.org/10.1016/j.electacta.2016.01.051

Table 2
Individual bands and the corresponding vibrational position in the Raman spectra of the different types of sol gel glass studied. (L) is low intensity; (B) is broad peak and (S) shoulder.

	TMS	SS_TMS_58S t = 0	SS_TMS_58S-a t = 0	SS_TMS_58S t = 17 d	SS_TMS_58S-a t = 17 d
Tetrasiloxane	485	485	485	486	485
rings	607(L)	606(L)	606(L)	606	606
Si-O ring defects	794	715(B L)	712(B L)	606	606
P-O-P		748(B L)	748(B L)	761	761
Ca-NO_3				912	912
Ca-NO_3				1030	1028
O-Si-O bridge					
Si-O-Si symm stretch					
Si-(OH)					
Si-O structural bridging					
-NO_3	1169	1053	1055*	1049*	1049*
-CH_3 rocking	1245	1076(S)	1065*	1057(S)*	1056(S)*
Si-O-Si network		1170	1168	1184	1184
Si-CH_3		1242	1240(B)	1245	1248
P = O				1297	1297

and an important drop of the phase angle in the high frequency that can be related to the defects created in the film that allows the entrance of the electrolyte in the defects of the coating.

The interpretation of the experimental data of the impedance spectra with an electrical model of the metal/coating interface, can lead to a better insight of the deterioration pathway. In this work Constant Phase Elements (CPE) instead of capacitances were used when phase angle was different from −90°. The impedance for the CPE, Z_{CPE}, element can be written as [26]:

$$Z_{CPE} = \frac{1}{Q(j\omega)^{\alpha}} \quad (1)$$

where Q (pseudocapacitance) and α are the CPE parameters, independent of frequency, j is the current density and ω the frequency.

The CPE is generally attributed to distributed surface reactivity, surface inhomogeneity, roughness or fractal geometry, electrode porosity, and to current and potential distributions associated with electrode geometry [27]. As Q cannot represent the capacitance when $\alpha < 1$, it can be related with the effective capacity (Ceff) of the analyzed coating, applying a surface distribution of the elements, which leads eq. 3 [28].

$$Ceff = Q^{1/\alpha}\left(\frac{Rsol.Rcoat}{Rsol + Rcoat}\right)^{\frac{1-\alpha}{\alpha}} \quad (3)$$

Rsol is the solution or medium resistance and Rcoat is the coating resistance. In the present work Ceff was calculated for the high frequency part of the impedance spectra [29], assuming a parallel array between the CPE of the coating and the Rcoat in the electric circuits. Fig. 7 shows the Ceff for the coatings calculated for the coated samples immediately after immersion and after 17 days of immersion, considering a parallel arrangement of the CPEcoat and Rcoat. The lowest effective capacity is for SS_TMS samples showing an isolating and protective film. The SS_TMS_58S coating show and increase in its Ceff with immersion but this increase in lower than for the SS_TMS_58S-a evidencing that the deterioration of the film is

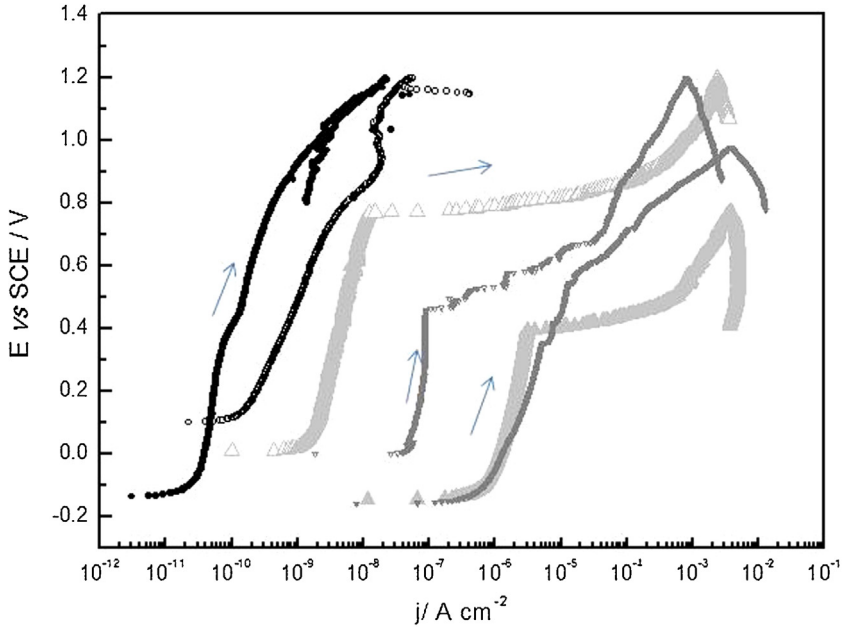

Fig. 5. Potentiodynamic polarization curves for the coated samples immediately after immersion and after immersion. (●) SS_TMS; (▲) SS_TMS_58S; (▼) SS_TMS_58S-a. Full symbols represent after 17 days of immersion and empty symbols represents the just immersed samples. The arrows indicate the direction of sweeping potentials.

Please cite this article in press as: S.A. Omar, et al., Protection and functionalization of AISI 316L stainless steel for orthopedic implants: hybrid coating and sol gel glasses by spray to promote bioactivity, Electrochim. Acta (2016), http://dx.doi.org/10.1016/j.electacta.2016.01.051

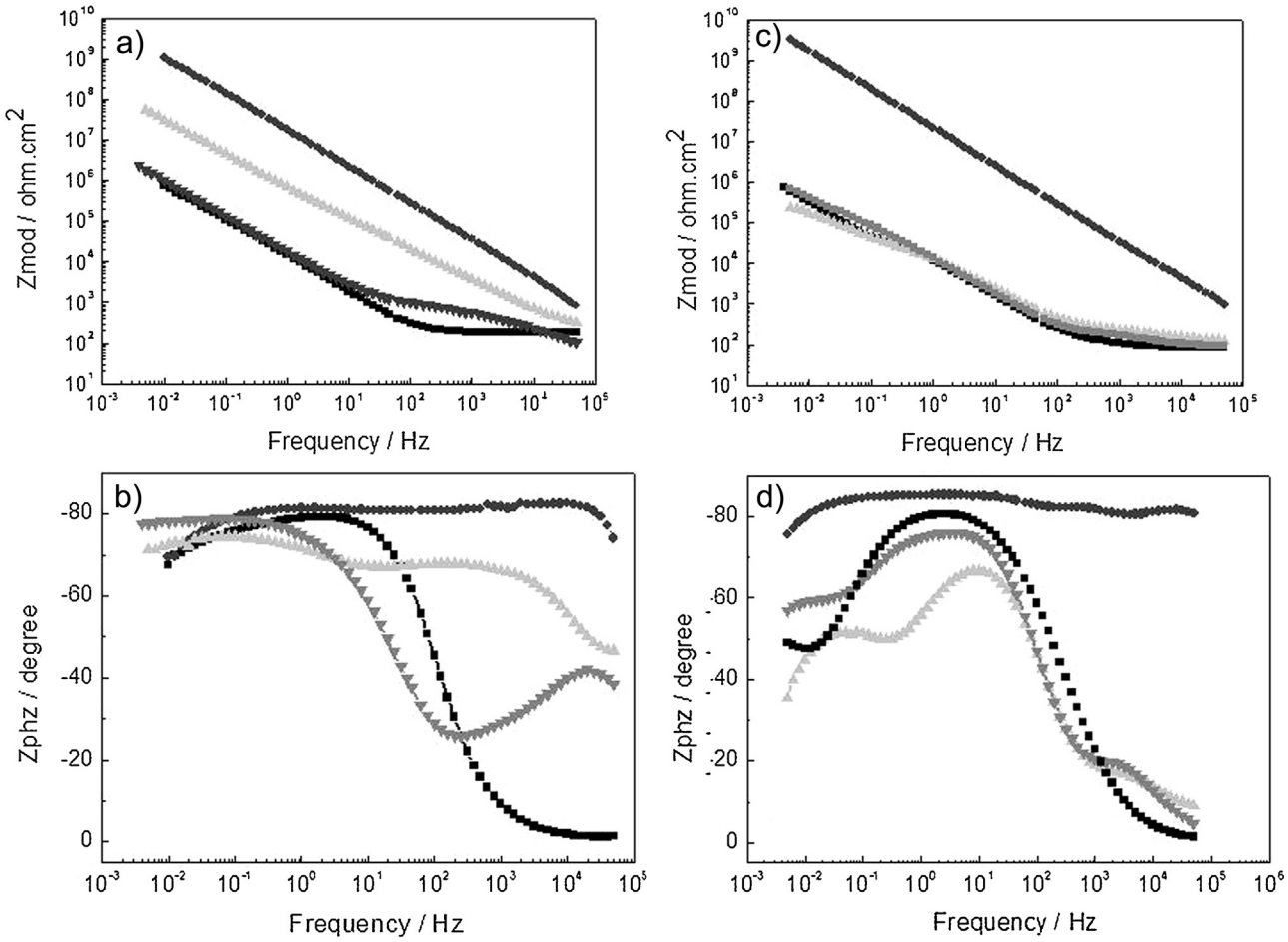

Fig. 6. Bode representation of impedance assays at immediately after immersion (a and b) and after 17 days of immersion (c and d) in SBF. (■) SS; (●) SS_TMS; (▲) SS_TMS_58S; (▼) SS_TMS_58S-a.

bigger for the SS_TMS_58S-a condition behaving as a leaky capacitor non being efficient as protection for the substrate. This fact is noticeable from Fig. 3 where cracks can be seen on the surface before immersion and after immersion, the dissolution of the particles occurs and the defects seem to increase. The variation of Rcoat can be observed in Fig. 8, where the low values for Rcoat for SS_TMS_58S-a at both immersion times denotes the existence of electrolyte pathways from the beginning of immersion. The decrease in Rcoat is also noticeable for the other coatings but the TMS coating (shown in the insert) presents a two orders of magnitude higher value of resistance that the other coatings systems showing a better surface coverage and isolating properties.

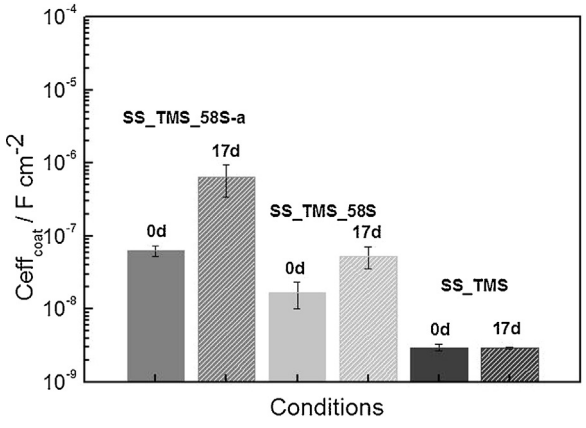

Fig. 7. C_{eff} for the coatings calculated according to eq 3 for the coated samples immediately after immersion and after 17 days of immersion.

4. Conclusions

Sol-gel TMS coating applied onto stainless steel supplies an enhancement in the corrosion resistance when compare with bare metal in SBF, being a useful film with protective purposes. The addition of 58S bioactive particles by spray method results appealing as it is a simple way to generate bioactive points on the implant surface; however the application denotes a loss on its corrosion resistance. Even there is a hint of some kind of detrimental effect regarding the corrosion behavior between the bioactive dots and the TMS coating, the entire system SS_TMS_58S results promising for further investigation.

Acknowledgments

The support from the Consejo Nacional de Investigaciones Científicas y Técnicas (CONICET) and the Universidad Nacional de Mar del Plata (UNMdP), Argentina is gratefully acknowledged. The

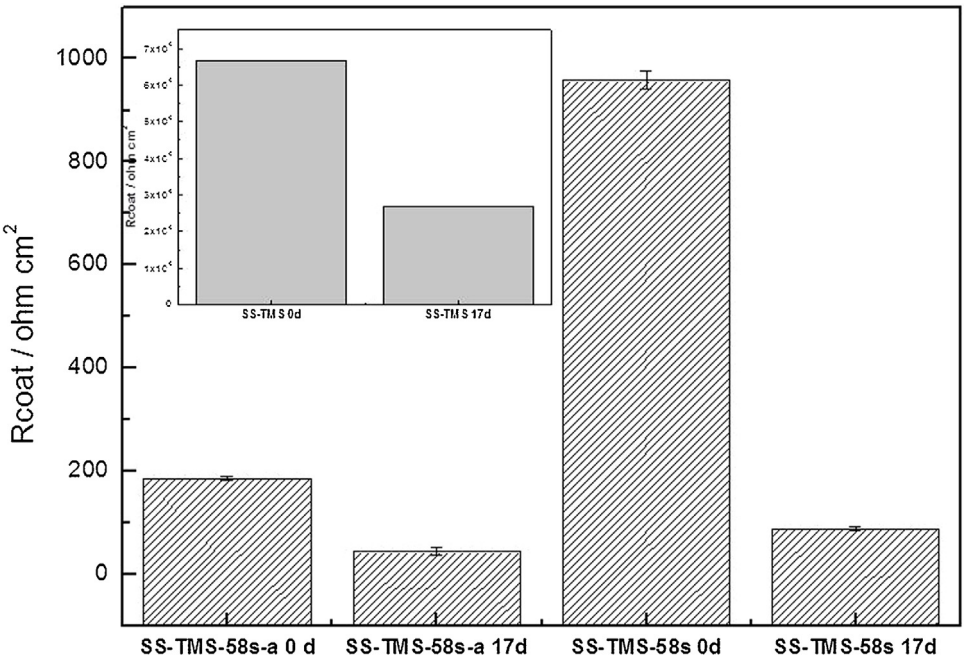

Fig. 8. Rcoat for the coated samples considering a parallel arrangement with the CPEcoat. In the insert the values for SS-TMSo.

authors also acknowledge Dr. Desimone (INTEMA, Argentina) by her support on Raman measurements.

References

[1] C. Brinker, A.J. Hurd, K.J. Ward, G.C. Frye, K.J. Ward, C.S. Ashley, Sol-gel thin film formation, Journal of Non-Crystalline Solids. 121 (1990) 294–302.
[2] M. Guglielmi, Rivestimenti sottili mediante dip coating con metodo sol-gel, Revista della Staz. Sper. 4 (1988) 197–199.
[3] C. Sanchez, M. In, Molecular design of alkoxide precursors for the synthesis of hybrid organic-inorganic gels, Journal of Non-Crystalline Solids 147-148 (1992) 1–12.
[4] O. de Sanctis, L. Gomez, N. Pellegri, C. Parodi, A. Marajofsky, A. Duran, Protective glass coatings on metallic substrates, Journal of Non-Crystalline Solids 121 (1990) 338–343.
[5] N. Pellegri, O. Sanctis, A. Durán, Preparation and microstructure study of borosilicate coatings produced by sol-gel, Journal of Sol-Gel Science and Technology 2 (1994) 519–523.
[6] A. Rámila, F. Balas, M. Vallet-Regí, Synthesis routes for bioactive sol-gel glasses: Alkoxides versus nitrates, Chemistry of Materials 14 (2002) 542–548.
[7] I. Izquierdo-Barba, A.J. Salinas, M. Vallet-Regí, Bioactive Glasses: From Macro to Nano, International Journal of Applied Glass Science 4 (2013) 149–161.
[8] M. Cerruti, G. Magnacca, V. Bolis, C. Morterra, Characterization of sol-gel bioglasses with the use of simple model systems: A surface-chemistry approach, Journal of Materials Chemistry 13 (2003) 1279–1286.
[9] Zplot for Windows, Electrochem. Impedance Software Operating Manual, Part 1 Scribner Ass. Inc. Southern Pines, NC (1998).
[10] J. Ballarre, D.A. López, W.H. Schreiner, A. Durán, S.M. Ceré, Protective hybrid sol-gel coatings containing bioactive particles on surgical grade stainless steel: Surface characterization, Appl Surf Sci 253 (2007) 7260–7264.
[11] L. Todan, E.M. Anghel, P. Osiceanu, R.V.F. Turcu, I. Atkinson, S. Simon, M. Zaharescu, Structural characterization of some sol-gel derived phosphosilicate glasses, Journal of Molecular Structure 1086 (2015) 161–171.
[12] F. Bonino, A. Damin, V. Aina, M. Miola, E. Vernè, O. Bretcanu, S. Bordiga, A. Zecchina, C. Morterra, In situ Raman study to monitor bioactive glasses reactivity, Journal of Raman Spectroscopy 39 (2008) 260–264.
[13] T.T. To, D. Bougeard, K.S. Smirnov, Molecular dynamics study of the vibrational pattern of ring structures in the Raman spectra of vitreous silica, Journal of Raman Spectroscopy 39 (2008) 1869–1877.
[14] M.C. Matos, L.M. Ilharco, R.M. Almeida, The evolution of TEOS to silica gel and glass by vibrational spectroscopy, Journal of Non-Crystalline Solids 147-148 (1992) 232–237.
[15] J. Yang, J. Chen, J. Song, Studies of the surface wettability and hydrothermal stability of methyl-modified silica films by FT-IR and Raman spectra, Vibrational Spectroscopy 50 (2009) 178–184.
[16] I.I. Kondilenko, P.A. Korotkov, N.G. Golubeva, Effect of water of crystallization on spontaneous Raman spectrum of calcium and magnesium nitrates, Journal of Applied Spectroscopy 20 (1975) 775–779.
[17] V.S. Naumov, Study of sodium interaction with calcium nitrate and carbonate in alkali metal chloride melts by IR and raman spectroscopy, Russian Journal of Inorganic Chemistry 55 (2010) 1202–1208.
[18] V.K. Mishra, B.N. Bhattacharjee, O. Parkash, D. Kumar, S.B. Rai, Mg-doped hydroxyapatite nanoplates for biomedical applications: A surfactant assisted microwave synthesis and spectroscopic investigations, Journal of Alloys and Compounds 614 (2014) 283–288.
[19] D. Arcos, D.C. Greenspan, M. Vallet-Regí, A new quantitative method to evaluate the in vitro bioactivity of melt and sol-gel-derived silicate glasses, Journal of Biomedical Materials Research - Part A 65 (2003) 344–351.
[20] R.A. Martin, S. Yue, J.V. Hanna, P.D. Lee, R.J. Newport, M.E. Smith, J.R. Jones, Characterizing the hierarchical structures of bioactive sol-gel silicate glass and hybrid scaffolds for bone regeneration, Philosophical Transactions of the Royal Society A: Mathematical, Physical and Engineering Sciences 370 (2012) 1422–1443.
[21] R.K. Brow, Review: the structure of simple phosphate glasses, J. Non-Cryst. Solids 263 (2000) 1–28.
[22] A. Bertoluzza, C. Fagnano, M. Antonietta Morelli, V. Gottardi, M. Guglielmi, Proceedings of the International Workshop on Glasses and Glass Ceramics from Gels Raman and infrared spectra on silica gel evolving toward glass, Journal of Non-Crystalline Solids 48 (1982) 117–128.
[23] A. Balamurugan, G. Sockalingum, J. Michel, J. Fauré, V. Banchet, L. Wortham, S. Bouthors, D. Laurent-Maquin, G. Balossier, Synthesis and characterisation of sol gel derived bioactive glass for biomedical applications, Materials Letters 60 (2006) 3752–3757.
[24] L.L. Hench, E.C. Ethridge, An interfacial approach, Academic Press Pennsylvania (1982) 384.
[25] F. Andreatta, L. Paussa, P. Aldighieri, A. Lanzutti, D. Raps, L. Fedrizzi, Corrosion behaviour of sol–gel treated and painted AA2024 aluminium alloy, Progress in Organic Coatings 69 (2010) 133–142.
[26] C.H. Hsu, F. Mansfeld, Technical note: Concerning the conversion of the constant phase element parameter Y0 into a capacitance, Corrosion NACE 57 (2001) 747–748.
[27] J.B. Jorcin, M.E. Orazem, N. Pébère, B. Tribollet, CPE analysis by local electrochemical impedance spectroscopy, Electrochimica Acta 51 (2006) 1473–1479.
[28] B. Hirschorn, M.E. Orazem, B. Tribollet, V. Vivier, I. Frateur, M. Musiani, Determination of effective capacitance and film thickness from constant-phase-element parameters, Electrochimica Acta 55 (2010) 6218–6227.
[29] P.L. Bonora, F. Deflorian, L. Fedrizzi, Electrochemical impedance spectroscopy as a tool for investigating underpaint corrosion, Electrochimica acta 41 (1996) 1073–1082.

Please cite this article in press as: S.A. Omar, et al., Protection and functionalization of AISI 316L stainless steel for orthopedic implants: hybrid coating and sol gel glasses by spray to promote bioactivity, Electrochim. Acta (2016), http://dx.doi.org/10.1016/j.electacta.2016.01.051